Computer Models of Watershed Hydrology

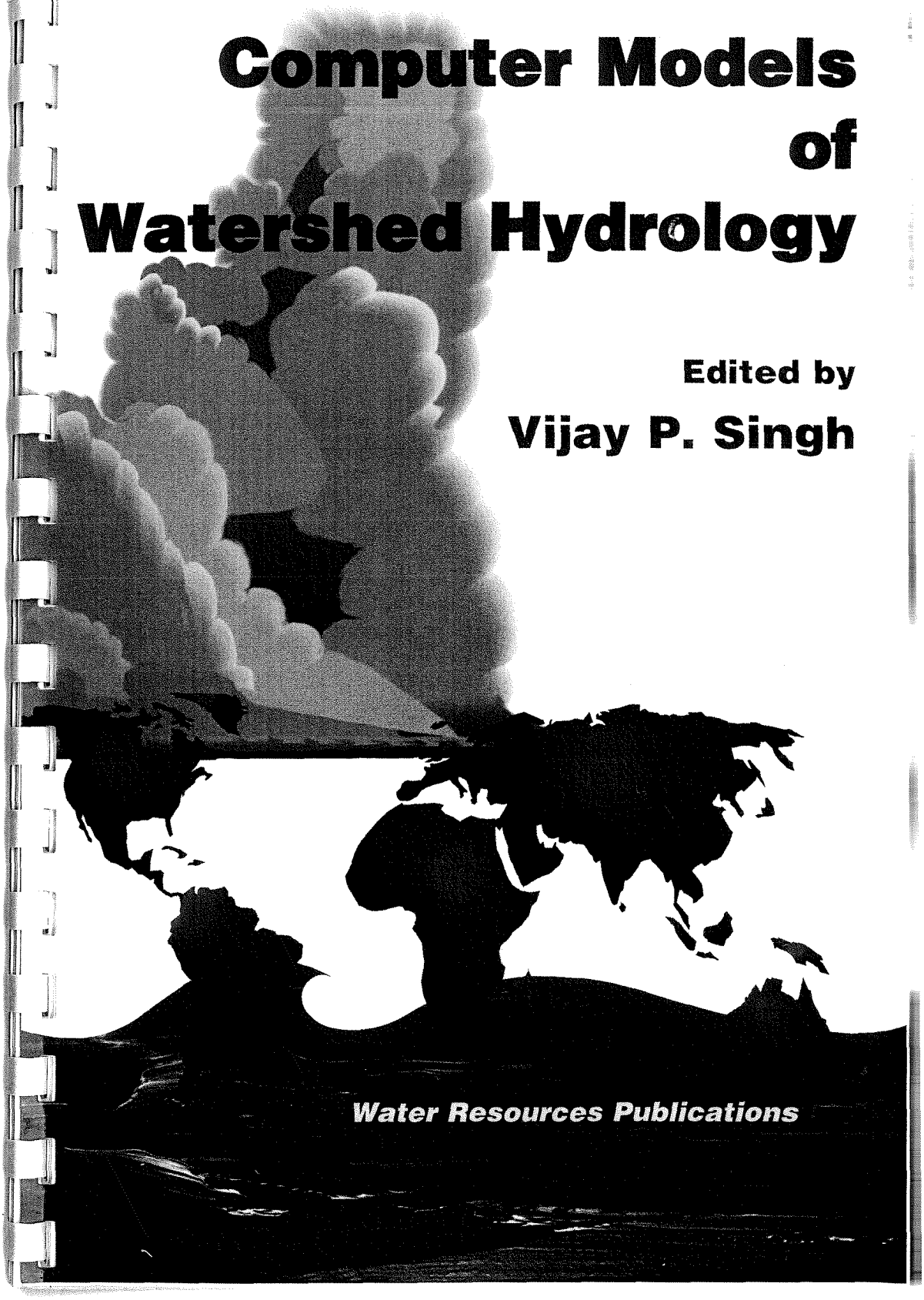

Edited by

Vijay P. Singh

Water Resources Publications

Chapter 20

KINEROS - A KINEMATIC RUNOFF AND EROSION MODEL

R.E. Smith, D.C. Goodrich, D.A. Woolhiser, and C.L. Unkrich

20.1. INTRODUCTION

KINEROS, an acronym for KINematic runoff and EROSion model, has evolved over a number of years primarily as a research tool. However some consulting firms have been attracted by several of its unique features and KINEROS has been used as an engineering tool in the U.S. and abroad.

The logical structure on which KINEROS is based, routing surface runoff over cascades of overland flow planes contributing lateral inflow to channels, was developed in the late 1960's (Woolhiser, et al. 1970). An interactive infiltration component was added by Rovey (1974) and the program, known then as KINGEN, was documented and released (Rovey, et al. 1977). The model was tested with data from the CSU Outdoor Experimental Rainfall-Runoff Facility (Dickinson et al. 1967), agricultural plots and small watersheds, and with urban runoff data. After the release of KINGEN, several modifications were made, including the addition of an erosion and sediment transport component, modification of the infiltration component, addition of a pond element, and modification of the input to allow spatial variability of rainfall. These modifications were incorporated into a model called KINEROS and were documented and released (Woolhiser, et al. 1990a). Since then, KINEROS was modified to account for small scale spatial variation of saturated conductivity. This version of KINEROS was subjected to rigorous testing on split sample data from semiarid watersheds ranging from 1.5 to 630 ha. (Goodrich 1991, Woolhiser et al. 1990b, Michaud, 1992). The results were very encouraging for basins up to about 3 sq. mi. (760 ha.) and demonstrated the necessity of accounting for small scale spatial variability of saturated conductivity and rainfall. These studies also emphasized the importance of carefully checking the experimental rainfall-runoff data to prevent misleading conclusions regarding model applicability.

The following discussion provides an overview of the theory and structure of KINEROS and an analysis of model results. First, the basic theory and assumptions of the processes are presented. Next, the results of testing of KINEROS are presented. Finally, a description of improvements underway will be presented.

20.2. KINEROS BASIC STRUCTURE

20.2.1. Representation of Catchment Geometry

The KINEROS model user must transform the catchment of interest into an equivalent network composed of runoff surfaces or "planes", intercepting channels (or conduits in the case of urban storm drains), and ponds or detention storages. Each of these is oriented such that 1-dimensional flow can be assumed, and each such unit is termed an *element* of the overall network. Figure 20.1 illustrates schematically and conceptually the major

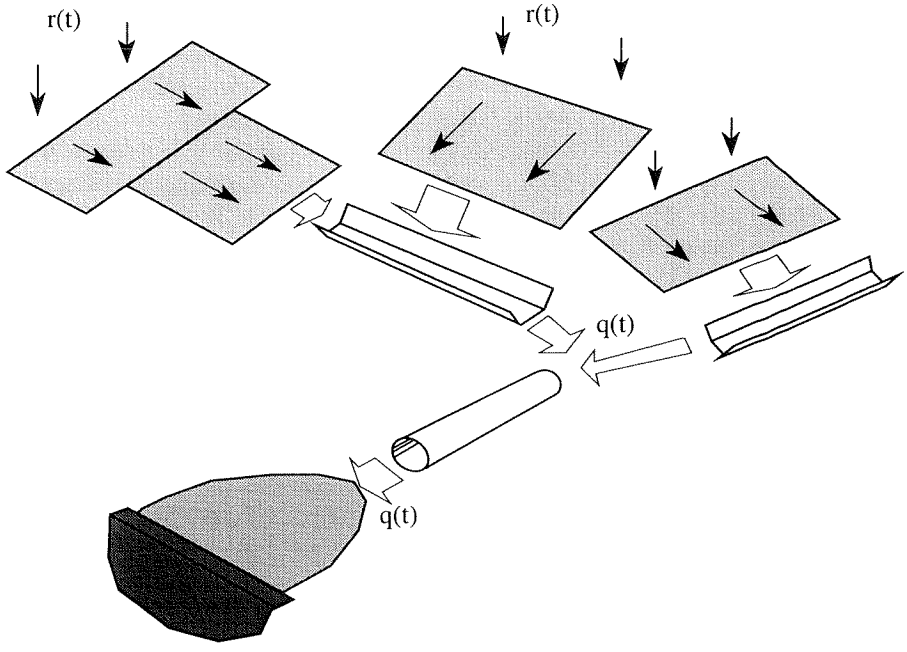

Fig. 20.1. Schematic example of various hydrologic elements used in KINEROS, and some of the ways that they may be interconnected to represent urban or rural watersheds.

types of elements and their connections. The User Manual (Woolhiser et al, 1990a) gives examples to aid in this geometric simplification. Runoff surfaces may be composed of a cascade of rectangular surfaces, which allows the simulation of converging flow areas, or areas of nonuniform slope, hydraulic resistance, or soils. Hortonian runoff is then simulated for the network of elements, culminating in the production of a simulated hydrograph at the outlet. The processes simulated, and the equations involved, will be described in general order of occurrence in the runoff - erosion generation process.

20.2.2. Rainfall Excess Calculation

20.2.2.1. Distributed Rainfall Data. Rainfall information for as many as 20 gage sites within or adjacent to the basin may be provided for use in the model. KINEROS requires information in the form of accumulated depth / time pairs, and converts this data into rainfall rate pulses. The raingages are identified by number, and input data must indicate which gage is associated with each catchment element. A gage weighting factor may be used to adjust the data from a gage for the associated element.

20.2.2.2. Interception. A total depth of interception may be specified for each runoff element, based on the vegetation or other surface condition. This amount is taken from the earliest rainfall pulses until the potential interception depth is filled. The modified rainfall pulse data then becomes input to the soil surface.

20.2.2.3. Infiltration during rainfall. As will be discussed later, each flow element is divided along its flow path into computational finite increments separated by nodes. The rainfall excess rate at a computational node for each surface element is found by the difference between the rainfall rate and the rate at which the soil can absorb or infiltrate rainfall. Soil water infiltration varies considerably in time depending on both soil hydraulic parameters and other time-varying soil conditions. The infiltration model used in KINEROS (Smith and Parlange, 1978) is based on an approximate solution of the basic equation of unsaturated flow. The model requires three parameters to describe the infiltration behavior of the soil during a rainfall event. $f_c = f(I, \theta_i)$

Infiltration capacity, f_c, is the maximum rate at which water can enter the soil surface. It is always determined by soil properties and water content of the soil. In KINEROS, it is described as a function of two variables: $f_c = f(I,\theta_i)$, where I is the cumulative amount of infiltrated water, starting at the beginning of the storm, when initial water in the soil profile, θ_i, is assumed uniform. f_c is also a function of three primary soil parameters, G, S_i, and K_s, which will be discussed below. Unless rainfall rate exceeds the

infiltration capacity, the infiltration rate at any time during a rainstorm is limited by the rainfall rate r,

$$f = Min[f_c, r] \tag{20.1}$$

and this definition of f leads to the definition of I;

$$I = \int_o^t f dt \quad . \tag{20.2}$$

I is the independent variable for the infiltration capacity, f_c (Smith and Parlange, 1978),

$$f_c = K_s \frac{\exp(I/B)}{\exp(I/B)-1} \tag{20.3}$$

in which K_s is the surface soil effective saturated hydraulic conductivity, cm/min and B is a term combining a capillary drive parameter and the soil saturation deficit,

$$B = (\theta_s - \theta_i) G \quad . \tag{20.4}$$

These equations describe an implicit relation, but solution is not difficult, as discussed below. Initial water content θ can vary from 0 (in theory) to a maximum value, θ_s, slightly less than the soil porosity. Soils exhibit a rapidly decreasing relative hydraulic conductivity, $k_r = K/K_s$, as soil water tension is increased (or as soil capillary head, ψ, decreases). The effective capillary drive, G, reflects the soil's capillary properties. G is defined by the integral of the unsaturated relative hydraulic conductivity function for the soil.

$$G = \int_{-\infty}^{0} k_r(\psi) d\psi \quad . \tag{20.5}$$

Estimated values for the parameters G and K_s for a variety of soil textural classes have been determined by statistical study of measured data (Rawls et al. 1982) and are furnished in the KINEROS User Manual. It should be noted that the parameters have substantial variability within textural classes, so that values obtained from the tables should be considered as "starting values" only.

The parameter θ_s is usually slightly below the soil porosity ϕ and is not difficult to determine since it has a small range. The saturation deficit (θ_s -

θ_i) is actually one parameter, because θ_s is fixed from storm to storm (except for cultivated soils). For ease of estimation, the KINEROS input parameter for soil water is a scaled water content, $S = \theta/\phi$, (ϕ is the soil porosity) which varies from 0 to 1. Thus initital soil conditions are represented by the variable S_i ($= \theta_i/\phi$).. In KINEROS, S_{max} is the scaled equivalent of θ_s. S_i cannot be as great as S_{max}, and is usually limited at the lower end not by 0 but by a residual saturation S_r. S_r conceptually represents that water which cannot be removed from the soil by capillary forces, but is often merely a fitting parameter for soil data. The parameter S_r is used in soil water redistribution during breaks in a rainfall sequence. Thus, there are two parameters, K_s, and G to characterize the soil, and the variable S_i to characterize the initial condition. Although in practice, the parameters K_s and G are often treated as constants, they are affected by tillage operations and biological activities between rainfall events.

While Eq. (20.3) is not explicitly a function of time, it can be transformed into a time dependent function. The advantage of I as an independent variable is that Eq. (20.3) describes in one expression both the occurrence of ponding and the decay of f_c after ponding (Smith, 1982).

Figure 20.2 shows the relation f(I) represented by Eq. (20.3). Actual infiltration is the shaded part. As this figure shows, I is accumulated as $\sum rdt$ until the limit described in Eq. (20.3) is reached, after which I is accumulated as described by Eqs. (20.2) and (20.3).

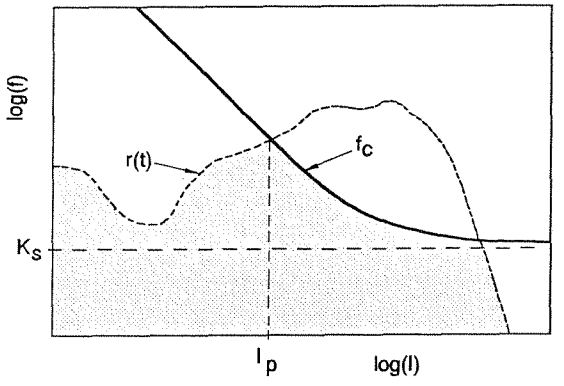

Fig. 20.2. Schematic of the "universal" relation of infiltration rate to infiltrated volume, and to infiltration capacity, f_c.

20.2.2.4. Infiltration during recession. Infiltration calculations should continue after rainfall slows or ceases as long as there is water on the soil surface. This implies a further interaction between the infiltration model and the surface flow model. During recession, however, it is not assumed that the entire surface is covered with water. KINEROS assumes a

relatively simple relation between mean surface water depth, h, and the proportion of the surface covered, p_{rc}, at any location along the flow direction, such that $p_{rc} = h/h_c$ [for $h < h_c$]. h_c is accepted as a recession parameter for each surface element.

20.2.2.5. Recovery of infiltration capacity during an interruption. The infiltration theory summarized above may be used for any value of $r > K_s$. When r falls below K_s, but is greater than 0, the surface soil water content will approach a value which is dependent on r, and this asymptotic value $S_*(r)$ can be estimated by a function

$$S_*(r) = S_r + (S_{\max} - S_r)\left[\frac{r}{K_s}\right]^p \qquad (r < K_s) \tag{20.6}$$

In theory, the parameter p varies with soil type, but is taken as constant in KINEROS for simplicity. KINEROS assumes that during a break in rainfall S_* is approached asymptotically, and that the value of S_* cannot be less than a user supplied estimate of "field capacity". Estimates are supplied in the User Manual. The asymptote is approached more rapidly for soils with large value of K_s, and more slowly for cases where I is large and when there is water on the surface. Mathematically, these concepts are described as

$$S_i^j = S_i^{j-1} + (S_* - S_i^{j-1})[1 - \exp(-\eta \Delta t)] \tag{20.7}$$

in which

$$\eta = [1 - h/h_c]\exp(-2I)\sqrt{aK_s} \tag{20.8}$$

and S_i^j is the relative saturation at node i for time step j. It should be pointed out that since the development of KINEROS, a relatively efficient and accurate theory for soil water redistribution and reinfiltration during storm intervals has been developed (Smith *et al.*, 1993), and will replace this approximate method in a new version of KINEROS.

20.2.2.6. Numerical Method of Solution. During a computational time interval $\Delta t(i)$, the appropriate value of f is its interval mean value

$$f = [I(t + \Delta t) - I(t)]/\Delta t \quad . \tag{20.9}$$

Prior to ponding, solution is direct, since f = r. After ponding, the value of f may be found by either numerical integration, or series approximation for the exponential function in Eq. (20.3), which leads to a time explicit function. For the period after ponding, KINEROS uses numerical

integration, solving the following equation in small subdivisions δt until $t+\Delta t$ is reached:

$$\Delta t = \int_{I(t)}^{I(t+\Delta t)} \frac{dI}{f_c(I)} \tag{20.10}$$

20.2.3. Hortonian Overland Flow

20.2.3.1. Basic Equations. After sufficient rainfall excess water appears on a surface to overcome surface tension and fill small surface depressions, overland flow begins. Viewed at a microscale, overland flow is an extremely complicated, multidimensional, and heterogenous process. At a larger scale, however, it can be usefully viewed as a one-dimensional flow process in which flux is a power function of the unit storage (storage per unit area, or mean depth of flow);

$$Q = \alpha h^m \tag{20.11}$$

where Q is the discharge per unit width, h is the unit storage of water (or mean depth for smooth surfaces), and α and m are parameters related to slope, surface roughness, and flow condition (laminar or turbulent flow). Equation (20.11) is used in conjunction with the equation of continuity,

$$\frac{\partial h}{\partial t} + \frac{\partial Q}{\partial x} = q(x,t) \tag{20.12}$$

where t is time, x is the distance coordinate, and q(x,t) is the rate of local input, or lateral inflow. For overland flow, Eq. (20.11) may be substituted into Eq. (20.12) to obtain

$$\frac{\partial h}{\partial t} + \alpha m h^{m-1} \frac{\partial h}{\partial x} = q(x,t) \tag{20.13}$$

A definition sketch of one-dimensional surface flow in response to a distributed input is shown in Fig. 20.3. It must be emphasized that KINEROS does not assume overland flow elements to be flat planes, but only assumes that Eq. (20.11) describes the normal flow process. This is all that is required by the kinematic assumption. High slopes or supercritical flow are not required.

The kinematic wave equations are simplifications of the de Saint Venant equations, and do not preserve all of the properties of the more complex equations, such as backwater and diffusive wave attenuation. Attenuation does occur in kinematic routing from shocks or from spatially variable

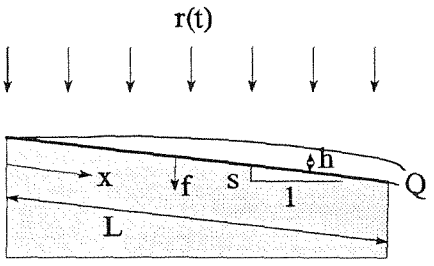

Fig. 20.3. Definition sketch of overland flow on an infiltrating surface.

infiltration. The kinematic routing method is an excellent approximation for most overland flow conditions (Woolhiser and Liggett 1967, Morris and Woolhiser 1980).

20.2.3.2. Boundary Conditions. The depth or unit storage at the upstream boundary must be specified to solve Eq. (20.13). If the upstream boundary is a flow divide, the boundary condition is

$$h(0,t) = 0 \tag{20.14}$$

If another surface is contributing flow at the upper boundary, the boundary condition is

$$h(0,t) = \left[\frac{\alpha_u h_u(L,t)^{m_u} W_u}{\alpha W}\right]^{1/m} \tag{20.15}$$

This merely states an equivalence of discharge, in terms of the values of h and the appropriate parameters at the bottom (length L) of the upstream element (subscript u) and at the upstream end of the element in question

20.2.3.3. Numerical Solution. KINEROS solves the kinematic wave equations using a four-point implicit method. Notation for this method is shown in Fig. 20.4, and the finite difference equation for Eqs. (20.11) and (20.12) is

$$\begin{aligned} &h_{j+1}^{i+1} - h_{j+1}^{i} + h_{j}^{i+1} - h_{j}^{i} + \\ &+\frac{2\Delta t}{\Delta x}\left\{\theta_w\left[\alpha_{j+1}^{i+1}\left(h^m\right)_{j+1}^{i+1} - \alpha_{j}^{i+1}\left(h^m\right)_{j}^{i+1}\right] + (1-\theta_w)\left[\alpha_{j+1}^{i}\left(h^m\right)_{j+1}^{i} - \alpha_{j}^{i}\left(h^m\right)_{j}^{i}\right]\right\} \\ &\qquad - \Delta t\left(\bar{q}_{j+1} + \bar{q}_{j}\right) = 0 \end{aligned} \tag{20.16}$$

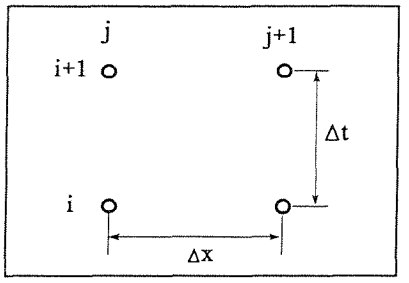

Fig. 20.4. Notation for the space and time dimensions of the finite difference grid.

where θ_w is a weighting parameter (usually 0.6 to 0.8) for the x derivatives at the advanced time step. A solution is obtained by Newton's method (sometimes referred to as the *Newton-Raphson* technique). While the solution is unconditionally stable in a linear sense, the accuracy is highly dependent on the size of Δx and Δt values used. The difference scheme is nominally of first order accuracy.

20.2.3.4. Roughness Relationships. Four options for α and m in Eq. (20.11) are provided in KINEROS:

1. The Manning hydraulic resistance law is used. In this option

$$\alpha = 1.49\frac{S^{1/2}}{n}, \quad \text{and} \quad m = 5/3 \tag{20.17}$$

where S is the slope, n is a Manning's roughness coefficient for overland flow, and English units are used. A table of values of n for use on surfaces are suggested in the User Manual.

2. A laminar law is used until the Reynolds number (R_e=Q/ν) exceeds a critical value (R_{cr}), and then Manning's law is used. Thus if R_e is smaller than R_{cr},

$$\alpha = \frac{8gS}{k\nu}, \quad \text{and} \quad m = 3 \tag{20.17}$$

where ν is the kinematic viscosity, g is the acceleration of gravity, and k is a dimensionless parameter that has a theoretical value of 24 for a hydraulically smooth surface and may be on the order of 14,000 for turf (Morgali 1970). If R_e is greater than R_{cr}, Eq. (20.17) is used.

3. A laminar law is used until the Reynolds number exceeds a critical value and then the Chezy law is used. Thus if R_e is smaller than R_{cr}, Eq. (20.18) is used. If R_e is greater than R_{cr},

$$\alpha = CS^{1/2}, \quad \text{and} \quad m = 3/2 \tag{20.19}$$

where C is the Chezy friction coefficient.

4. The Chezy law, Eq. (20.19), is used for all values of R_e.

Overland flow response characteristics are controlled by the slope, slope length, and hydraulic resistance parameters as well as the rainfall intensity and infiltration characteristics. For example, if the Manning resistance law is used, the time to equilibrium (t_e)[seconds] of a surface of length (L) and slope (S) with a constant rate of lateral inflow (q)[L/T], is

$$t_e = \left[\frac{nL}{1.49S^{1/2}q^{2/3}}\right]^{3/5} \tag{20.20}$$

where n is the Manning resistance coefficient. Therefore, to maintain the time response characteristics of the catchment we must retain the slope, slope length, and hydraulic resistance in our simplified version of a complex catchment. The length, width, and slope of the overland flow elements can be determined from topographic maps. The hydraulic resistance parameter is more difficult to determine. First, a decision must be made regarding the appropriate flow law. It is generally agreed that overland flow on a surface begins as laminar flow and eventually becomes turbulent at large Reynolds numbers. Values of the critical Reynolds number range from 100 to 1,000 (Chow 1959, Yu and McNown 1964, Morgali 1970). However, raindrops impacting on the water film generate local areas of turbulent flow and have an effect similar to increasing the viscosity of the fluid. For example, the relationship between the DarcyWeisbach friction factor (f_D) and Reynolds number for laminar flow over a hydraulically smooth surface is

$$f_D = \frac{24}{R_e} \quad . \tag{20.21}$$

Several laboratory experiments (cf. Glass and Smerdon 1967, Li 1972) have shown that with raindrop impact this relationship becomes

$$f_D = \frac{k}{R_e}; \qquad k > 24 \tag{20.22}$$
$$k = k_o + \chi(r)$$

where k_o is the appropriate value for a given surface geometry without raindrop impact and $\chi(r)$ is some function of the rainfall rate. Although the effects of raindrop impact can be significant on hydraulically smooth surfaces such as laboratory catchments, they are not important for hydraulically rough surfaces usually found in the field. The laminar flow model in KINEROS does not include a relationship between k and rainfall rate. Ranges of k_o for various surfaces are presented in the User Manual (Woolhiser et al. 1990).

Although the range of k_o for each surface is large, the time of equilibrium is proportional to $k_o^{1/3}$, so a 10 percent error in k_o will cause a smaller error in t_e. It should be noted that the relationship $R_e = Q / \nu = uh/ \nu$ is used for all surfaces in KINEROS although, for example, the local depth (h) may not be the appropriate characteristic length to use in flow through dense sod. In KINEROS the critical Reynolds number is calculated from the appropriate turbulent Manning's n or Chezy C specified in the input data. Ranges of Manning's n and Chezy C obtained from experiments reported in the literature are presented in the User Manual (Woolhiser et al. 1990a).

20.2.4. Channel Routing

20.2.4.1. Basic Equations. Unsteady, free surface flow in channels is also represented by the kinematic approximation to the equations of unsteady, gradually varied flow. As indicated in Fig. 20.1, channel segments may receive uniformly distributed but time-varying lateral inflow from overland flow elements on either or both sides of the channel, from one or two channels at the upstream boundary, or from an area at the upstream boundary. The dimensions of overland flow units are chosen to completely cover the watershed, so rainfall on the channel is not considered directly. The continuity equation for a channel with lateral inflow is

$$\frac{\partial A}{\partial t} + \frac{\partial Q}{\partial x} = q_c(x,t) \tag{20.23}$$

where A is the cross-sectional area, Q is the channel discharge, and $q_c(x,t)$ is the net lateral inflow per unit length of channel. Under the kinematic assumption, Q can be expressed as a unique function of A and Eq. (20.23) can be rewritten as

$$\frac{\partial A}{\partial t} + \frac{\partial Q}{\partial A}\frac{\partial A}{\partial x} = q_c(x,t) \tag{20.24}$$

The kinematic assumption is embodied in the relationship between channel discharge and cross-sectional area such that

$$Q = \alpha R^{m-1} A \tag{20.25}$$

where R is the hydraulic radius. If the Chezy relationship is used, $\alpha = CS^{1/2}$ and m = 3/2. If the Manning equation is used, $\alpha = 1.49S^{1/2}/n$ and m = 5/3. Channel cross sections may be approximated as trapezoidal or circular, as shown in Fig. 20.5.

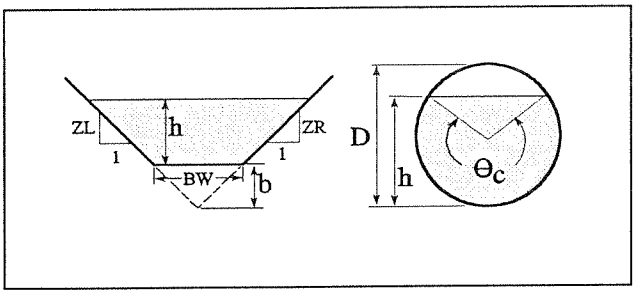

Fig. 20.5. Definition diagrams for a trapezoidal channel (left), and a channel conduit (right).

20.2.4.2. Circular Conduits. In an urban environment, circular conduits must be used to represent storm sewers. To apply the kinematic model, there must be no backwater, and the conduit is assumed to maintain free surface flow conditions at all times--there can be no pressurization. The continuity equation for a circular conduit is the same as Eq. (20.24) with $q_c = 0$. That is, there is no lateral inflow. The upper boundary condition is a specified discharge as a function of time. The most general discharge relationship and the one often used for flow in pipes is the Darcy-Weisbach formula,

$$S_f = \frac{f_D}{4R} \frac{u^2}{2g} \tag{20.26}$$

where S_f is the friction slope, f_D is the Darcy-Weisbach friction factor, and u is the velocity (Q/A). Under the kinematic assumption, the conduit slope S may be substituted for S_f in Eq. (20.26), so that

$$u = 2\sqrt{\frac{2g}{f_D} RS} \quad . \tag{20.27}$$

Discharge is computed by using Eq. (20.27), and a modification of Eq. (20.25),

$$Q = \frac{\alpha A^m}{p^{m-1}} \tag{20.28}$$

where p is the wetted perimeter, α is $[8gS/f_D]^{1/2}$, and m = 3/2. A schematic drawing of a partially full circular section is shown in Fig. 20.5. Geometric relationships for partially full conduits are further discussed in the documentation [Woolhiser et al. (1990a)].

20.2.4.3. Numerical Method for Channels. The kinematic equations for channels are solved by a four point implicit technique similar to that for overland flow surfaces, except that A is used instead of h, and the geometric changes with depth must be considered:

$$\begin{aligned} &A_{j+1}^{i+1} - A_{j+1}^{i} + A_{j}^{i+1} - A_{j}^{i} + \\ &+\frac{2\Delta t}{\Delta x}\left\{\theta_w\left[\frac{dQ^{i+1}}{dA}\left(A_{j+1}^{i+1} - A_{j}^{i+1}\right)\right] + \left(1-\theta_w\right)\left[\frac{dQ^{i}}{dA}\left(A_{j+1}^{i} - A_{j}^{i}\right)\right]\right\} \\ &-0.5\Delta t\left(q_{cj+1}^{i+1} + q_{cj}^{i+1} + q_{cj+1}^{i} + q_{cj}^{i}\right) = 0 \end{aligned} \tag{20.29}$$

where θ_W is a weighting factor for the space derivative. The terms dQ/dA are dependent only on channel geometry. Newton's iterative technique is used to solve for the unknown area A_{j+1}^{i+1}. The finite difference equation for circular conduits is the same as Eq. (20.29) except that the lateral inflow terms (q_c) are zero.

The appropriate value of Manning's n or Chezy C to use for channels in KINEROS depends on (1) the channel material (that is, grassed waterway, gravel bedded stream, concrete-lined channel), (2) the degree to which the channel conforms to the idealized trapezoidal cross section, and (3) how straight the channel reach is. Because of these factors, choice of the appropriate parameters is highly subjective, except for artificial channels. Barnes (1967) estimated Manning's n for several streams and presented pictures of the stream reaches. These photographs are very useful in obtaining estimates for natural channels. Values of Manning's n or Chezy C for artificial channels can be obtained from several sources, including Chow (1959).

In arid and semiarid regions, infiltration into channel alluvium may significantly affect runoff volumes and peak discharge. If the channel infiltration option is selected, Eq. (20.3) is used to calculate accumulated infiltration at each computational node, beginning either when lateral inflow begins or when an advancing front has reached that computational node.

Because the trapezoidal channel simplification introduces significant error in the area of channel covered by water at low flow rates (Unkrich and Osborn 1987), an empirical expression is used to estimate an "effective wetted perimeter." The equation used in KINEROS is

$$p_e = \min\left[\frac{h}{0.15\sqrt{BW}}, 1.0\right] p \qquad (20.30)$$

where p_e is the effective wetted perimeter for infiltration, h is the depth, BW is the bottom width, and p is the channel wetted perimeter at depth h. This equation states that p_e is smaller than p until a threshold depth is reached, and at depths greater than the threshold depth, p_e and p are identical. The channel loss rate is obtained by multiplying the infiltration rate by the effective wetted perimeter. Further experience may suggest changes in the form and parameters of Eq. (20.30).

20.2.5. Detention Structure Routing

In addition to surface and channel elements, a watershed may contain detention storage elements, which receive inflow from one or two channels and produce outflow from an uncontrolled outlet structure. This element can represent a pond, or a flume or other flow measuring structure with backwater storage. KINEROS accomodates up to three such elements. Rain falling on the pond and infiltration from the pond are not considered. As long as outflow is solely a function of water depth, the dynamics of the storage are well described by the mass balance and outflow equations,

$$\frac{dV}{dt} = q_t - q_o \qquad (20.31)$$

and

$$q_o = C_1(h_r - h_z)^{c_2} \qquad (20.32)$$

in which $V = V(h_r)$ is storage volume [L^3],

h_r = water surface elevation [L],

q_I = inf low rate [L^3 / T],

q_O = outflow rate [L^3 / T],

h_z = outflow weir or flume zero flow elevation [L], and

C_1 and c_2 = weir or orifice coefficients.

Water surface elevation (h_r) is measured from some datum below the lowest pond elevation, and $V(h_r)$ is determined from the description of the storage geometry. Equation (20.31) is written in finite difference form over a time interval (Δt) and the stage at time $t + \Delta t$ is determined by the bisection method. Equation (20.32) is general and can represent most control structures such as weirs, overfalls, or orifices. For weirs, C_1 must include the overfall length.

For purposes of water routing, the reservoir geometry may be described by a simple relationship between V, surface area, and h_r. Details for specification of detention pond geometry are given in the User Manual (Woolhiser et al. 1990a).

20.2.6. Surface Erosion and Sediment Transport

As an optional feature, KINEROS can simulate the movement of eroded soil along with the movement of surface water. KINEROS accounts separately for erosion caused by raindrop energy and erosion caused by flowing water, and continues the simulation through channel and pond elements. One necessary limitation is that, because a single mean particle size is used to characterize the eroded material, the effective soil particle size needs to be similar for all the eroding elements.

20.2.6.1. Upland Erosion. The general equation used in KINEROS to describe the sediment dynamics at any point along a surface flow path is a mass balance equation similar to that for kinematic water flow (Bennett 1974):

$$\frac{\partial(AC_s)}{\partial t} + \frac{\partial(QC_s)}{\partial x} - e(x,t) = q_c(x,t) \qquad (20.33)$$

in which C_s = sediment concentration $[L^3/L^3]$,

Q = water discharge rate $[L^3/T]$

A = cross sectional area of flow $[L^2]$,

e = rate of erosion of the soil bed $[L^2/T]$, and

q_s = rate of lateral sediment inflow for channels $[L^3/T/L]$.

For upland surfaces, e is assumed to be composed of two major components--production of eroded soil by splash of rainfall on bare soil, and hydraulic erosion (or deposition) due to the interplay between the shearing force of water on the loose soil bed and the tendency of soil particles to settle under the force of gravity. Thus e may be positive (increasing

concentration in the water) or negative (deposition). Net erosion is a sum of splash erosion rate as e_s and hydraulic erosion rate as e_h,

$$e = e_s + e_h \tag{20.34}$$

20.2.6.2. Splash Erosion. Based on limited experimental evidence, the splash erosion rate can be approximated as a function of the square of the rainfall rate (Meyer and Wischmeier 1969). This relationship can lead to physically unrealistic concentrations at the upstream boundary, so in KINEROS the splash erosion is somewhat modified as follows:

$$\begin{aligned} e_s &= c_f k(h) r q \quad ; \quad q > 0 \\ &= 0 \qquad\qquad ; \quad q < 0 \end{aligned} \tag{20.35}$$

in which c_f is a constant related to soil and surface properties, and k(h) is a reduction factor representing the reduction in splash erosion caused by increasing depth of water. Since q approaches r for high rainfall rates, this relation approximates the r^2 relation found by experiment except at the inception of runoff. k(h) is 1.0 prior to runoff and its minimum is 0 for very deep flow. The function k(h) is given by the empirical expression

$$k(h) = \exp(-c_h h) \tag{20.36}$$

The parameter c_h represents the damping effectiveness of surface water, and does not vary widely. Both c_f and k(h) are always positive, so e_s is always positive when there is rainfall and a positive rainfall excess (q).

20.2.6.3. Hydraulic Erosion. The hydraulic erosion rate e_h represents the rate of exchange of sediment between the flowing water and the soil over which it flows, and may be either positive or negative. KINEROS assumes that for any given surface water flow condition (velocity, depth, slope, etc.), there is an equilibrium concentration of sediment that can be carried if that flow continues steadily. Hydraulic erosion rate (e_h) is estimated as being linearly dependent on the difference between the equilibrium concentration and the current sediment concentration. In other words, hydraulic erosion/deposition is modeled as a kinetic transfer process;

$$e_h = c_g (C_{mx} - C_s) A \tag{20.37}$$

in which C_{mx} is the concentration at equilibrium transport capacity, C_s=C_s(x,t) is the current local sediment concentration, and c_g is a transfer rate coefficient [T^{-1}]. Clearly, the transport capacity is important in determining hydraulic erosion, as is the selection of transfer rate coefficient. Conceptually, when deposition is occurring, c_g can be shown to be equal to

the particle settling velocity, v_s, divided by the hydraulic depth, h. For erosion conditions on cohesive soils, the value of c_g must be reduced, and v_s/h is used as an upper limit for c_g.

20.2.6.4. Transport Capacity. Many transport capacity relations have been proposed in the literature, but most have been developed and tested for relatively deep, mildly sloping flow conditions, such as streams and flumes. In the absence of a clearly superior relation for shallow surface runoff, KINEROS provides the user a choice between several transport relationships. Julien and Simons (1985) showed that each could be represented by a generalized relation of the type

$$q_m = C_{mx}Q = \omega S^{\beta} Q^{\gamma} r^{\delta} \left[1 - \frac{\tau_c}{\tau_o}\right]^{\varepsilon} \quad ; \; \tau_o \geq \tau_c \tag{20.38}$$

in which q_m = transport capacity [L^2T^{-1}],

τ_o = bed shear stress [L /T],

τ_c = critical shear stress [L /T], and

ω = a coefficient.

Exponents ß, γ, and ε have values of either 0 or between 1 and 2, and ß varies from 0 to -2.24. Although not every transport relation selectable in KINEROS has non-zero values for all the exponents, ß, γ, and ε, all relations use local hydraulic conditions such as slope, velocity, or depth of flow. Some, in addition, use sediment specific gravity and the mean particle size of the soil rather than requiring selection of an empirical coefficient. The equations for each transport relationship are discussed in detail in the User Manual (Woolhiser et al. 1990a).

Particle settling velocity is calculated from particle size and density, assuming the particles have drag characteristics and terminal fall velocities similar to those of spheres (Fair and Geyer 1954). This relation is

$$v_s^2 = \frac{4}{3} \frac{g(S_s - 1)d}{C_D} \tag{20.39}$$

in which g = gravitational acceleration [LT^{-2}],

S_s = particle specific gravity,

C_D = drag coefficient, and

d = particle diameter [L].

The drag coefficient is a function of particle Reynolds number,

$$C_D = \frac{24}{R_n} + \frac{3}{\sqrt{R_n}} + 0.34 \tag{20.40}$$

in which R_n is the particle Reynolds number, defined as

$$R_n = \frac{v_s d}{\nu} \tag{20.41}$$

where ν is kinematic viscosity of water [L^2/T]. Settling velocity of a particle is found by solving Eqs. (20.39, 20.40, and 20.41) for v_s.

20.2.6.5. Numerical Method for Sediment Transport. Equations (20.33 - 20.37) are solved numerically at each time step used by the surface water flow equations. A four-point finite-difference scheme is used; however, iteration is not required since given current and immediate past values for A and Q and previous values for C_s, the finite difference form of this equation is explicit:

$$C_{s\,j+1}^{\,i+1} = f\left(C_{s\,j}^{\,i},\ C_{s\,j+1}^{\,i},\ and\ C_{s\,j}^{\,i+1}\right)$$

The value of C_{mx} is found from current hydraulic conditions.

20.2.6.6. Initial Conditions for Erosion. When runoff commences during a period when rainfall is creating splash erosion, the initial condition on the vector C_s should not be taken as zero. The initial sediment concentration at ponding ($C_s(t=t_p)$), can be found by simplifying Eq. (20.33) for conditions at that time. Variation with respect to x vanishes, and hydraulic erosion is zero. Then,

$$\frac{\partial(AC_s)}{\partial t} = e(x,t) = c_f rq - C_s v_s \tag{20.42}$$

where k(h) is assumed to be 1.0 since depth is zero. Since A is zero at time of ponding, and dA/dt is the rainfall excess rate (q), expanding the left-hand side of Eq. (20.42) results in

$$C_s(t=t_p) = \frac{c_f rq}{q + v_s} \tag{20.43}$$

The sediment concentration at the upper boundary of a single overland flow element, $C_s(0,t)$, is given by an expression identical to Eq. (20.43), and a similar expression is used at the upper boundary of a channel.

20.2.7. Channel Erosion and Sediment Transport

The general approach to sediment transport simulation for channels is nearly the same as that for upland areas. The major difference in the equations is that splash erosion (e_s) is neglected in channel flow, and the term q_s becomes important in representing lateral inflows. Equations (20.33) and (20.37) are equally applicable to either channel or distributed surface flow, but the choice of transport capacity relation may be different for the two flow conditions. For upland areas, q_s will be zero, whereas for channels it will be the important addition that comes with lateral inflow from surface elements. The close similarity of the treatment of the two types of elements allows the program to use the same algorithms for both types of elements.

The erosion computational scheme for any element uses the same time and space steps employed by the numerical solution of the surface water flow equations. In that context, Eqs. (20.33) and (20.37) are solved for $C_s(x,t)$, starting at the first node below the upstream boundary, and from the upstream conditions for channel elements. If there is no inflow at the upper end of the channel, the transport capacity at the upper node is zero and any lateral input of sediment will be subject there to deposition. The upper boundary condition is then

$$C_s(0,t) = \frac{q_s}{q_c + v_s BW} \tag{20.44}$$

where BW is the channel bottom width. A(x,t) and Q(x,t) are assumed known from the surface water solution.

20.2.8. Sediment Routing Through Detention Structures

For shallow rapid flow where erosion is generally more important than deposition, the use of a mean particle diameter can usually be justified for simulation purposes. When reservoirs are important elements in the catchment, however, KINEROS asks the user to specify a particle size distribution, because deposition is the only sedimentation process, and settling velocity is very sensitive to particle size. The distribution is characterized by a mean and a standard deviation and is assumed pseudonormally distributed into a number of particle size classes specified by the user.

The approach for pond sedimentation in KINEROS is similar to that for tank sedimentation, and particle fall velocities and flow-through velocities are used to find the trajectories that intersect the reservoir bottom. Particle fall velocities are calculated for each particle size class using Eqs. (20.39 and 20.41). Particles are assumed distributed uniformly through the reservoir depth in the first section at the inlet end, and the relative fall versus

lateral velocities from that point forward determine the proportion of each particle size class that deposits between successive cross sections. At successive sections, each particle size class will have a conceptual depth from the surface to the top of the area still containing sediment of that size.

Suspended and slowly falling particles are subject to molecular diffusion and dispersion, which can sometimes modify the time distribution of outflow concentrations. KINEROS simulates this modification using an effective dispersion coefficient, which is supplied by the user. Typical values suggested are from 10^{-5} to 10^{-4} ft^2/s. In many cases, dispersion is unimportant and can be neglected, such as for very short flow-through situations or for large particles. If a pond is located within a watershed, the mean particle diameter of the outflow will be smaller than that of the inflow. KINEROS cannot account for this phenomenon.

Since the time necessary for a reservoir outflow to approach zero may be significantly longer than that for a channel input hydrograph to return to zero, the user may need to specify a much longer simulation time if ponds are included in the catchment geometry.

20.3. EVALUATION OF KINEROS

20.3.1. Testing of KINEROS on the Colorado State University Outdoor Rainfall-Runoff Experimental Facility

The kinematic overland flow routing component of KINEROS and its precursors has been thoroughly tested using data from the Colorado State University Outdoor Rainfall-Runoff Experimental Facility (ORREF). This unique facility allows relatively precise measurement of rainfall and runoff at a scale comparable to small catchments, and has been described by Dickenson et al. (1967) and Woolhiser et al. (1971). The 0.2 ha (one-half acre) watershed consists of two parallelogram elements 35 m long contributing lateral inflow to a triangular channel 21.3 m long. A conical segment contributes runoff at the head of the channel. The overland flow elements have 5% slopes and the channel slope is 3%. Rainfall rates could be set at 12.5, 25, 50, and 100 mm/hr. The surface was covered with impervious butyl rubber and gravel was placed on the surface in various densities and spatial patterns to increase flow resistance.

Singh (1974) analyzed data from 210 experimental runs with 50 different configurations on the conical section and found that the kinematic wave formulation provided a good description of surface runoff from the facility. Singh (1974) used a numerical solution of the equations describing converging overland flow. Kibler and Woolhiser(1970) have demonstrated that the response of a converging section can be well approximated by the response of a cascade of rectangular surfaces as used in KINEROS.

Additional tests of the kinematic model using data from the ORREF were performed by Lane et al. (1975), Rovey, et al. (1977), and Wu et al. (1978), who also demonstrated that the flow measuring structure caused a lag in the measured rising hydrographs and that when this lag was accounted for, better agreement was achieved between measured and computed hydrographs. It should be pointed out that the researchers cited above used a second-order Lax-Wendroff numerical scheme which is more accurate than the current scheme in KINEROS. However if the guidelines in the KINEROS manual for choice of dx and dt increments are followed, there will be little difference in the numerical results.

20.3.2. Comparison to Other Models and Application on Small Watersheds

Zevenbergen and Peterson (1988) evaluated a variety of storm-event hydrologic and erosion models including a pre-release version of KINEROS (Woolhiser et al., 1990a). Also included in their evaluation were the following models: Areal Nonpoint Source Watershed Environmental Response Simulation (ANSWERS); Watershed and Sediment Runoff Simulation Model for Multiple Watersheds (MULTSED); Precipitation Runoff Modeling System (PRSM); and Hydrology and Sedimentology Watershed Model II (SEDIMOT, SEDCAD version). PRSM was not fully evaluated as it was primarily designed for continuous simulation.

A primary goal of the study was to judge the relative ability these models to predict sediment yield. There were three evaluation categories: "1) degree of physical process simulation; 2) how well the model results compare with observations at an instrumented watershed, and; 3) the sensitivity of model results to variations in input parameters." User manuals of the models were used to assess the type and number of physical processes treated in each model as well as watershed representation capability. They judged ANSWERS and KINEROS as allowing the greatest flexibility in watershed segmentation and MULTSED and KINEROS as simulating the greatest number of channel processes.

Each of the models was tested with runoff and sediment yield observations from nine storm events from a 1.9 ha (4.7 acre) experimental watershed in northwest Mississippi. The events ranged from small to quite large (ten year return period for two- and four-hour durations). Zevenbergen and Peterson (1988) graphically depicted runoff simulation ability of MULTSED, KINEROS and ANSWERS for one event and the agreement of the KINEROS simulation was judged to be "excellent," and slightly better than the simulations of the other two models. To evaluate sediment yield predictability, they calibrated detachment and transport coefficients on the second largest event and computed the coefficient of determination (CD) on the remaining eight events. Using the tractive force transport relation,

KINEROS had the highest CD (0.96) for sediment (CD = 1.0 represents perfect agreement). MULTSED also had a CD = 0.96 using the Meyer-Peter, Muller/Einstein relation. [A discrepancy pointed out by Zevenbergen and Peterson (1988) between ANSWERS and KINEROS using the Yalin transport relationship was due to a coding error in KINEROS which was corrected before the 1990 release.] The general conclusion of this study stated "that all the models except SEDIMOT are quite complementary with respect to hydrology and similar results can be achieved from ANSWERS, KINEROS or MULTSED models for sediment yield."

The KINEROS model has been applied to several semiarid watersheds covering a range of basin scales within the USDA-ARS Walnut Gulch Experimental Watershed operated by the Southwest Watershed Research Center in Tucson, AZ. A location map of the watershed and the specific subwatersheds discussed in this and the following section is presented in Fig. 20.6. Typical Walnut Gulch watershed characteristics include desert brush vegetation, sandy loam soils with significant rock content, and high amounts of soil surface erosion pavement. The subwatersheds are subject to high intensity precipitation from air-mass thunderstorms of limited spatial extent (Renard, 1970).

In February of 1981 the LH-6 (0.36 ha) watershed (see Fig. 20.6) was treated with the herbicide tebuthiuron to kill the woody plants, and was seeded with a mixture of grasses and forbes in June 1984. The adjacent LH-2 (1.4 ha) watershed was not treated with herbicide. KINEROS was used to model post-treatment events from LH-6 using parameters derived from pretreatment conditions (1973-1980) to assess whether the model would be able to detect changes in the runoff regime due to vegetation changes (see Woolhiser et al., 1990b for more detail). LH-2 was used for paired watershed comparisons between treated and untreated conditions.

Split sample calibration and verification of KINEROS using pretreatment runoff data was conducted to see if sufficient confidence could be gained in the model before it was used to attempt detection of vegetation change. Model performance for both calibration and verification was evaluated by inspection of individual hydrographs, examination of scatter plots of measured versus simulated runoff volumes and peak rates, and the coefficient of efficiency, E (Nash and Sutcliffe, 1970). E = 1 if the model predicts observed runoff with perfection. If E < 0, the model's predictive power is worse than simply using the average of observed values.

For the LH-6 watershed, 1:480 scale base maps indicated a representation with 23 overland flow elements and 7 channel elements (Fig. 20.6). The degree of topographic discretization is a central question in the application of a distributed model such as KINEROS. In many applications the channel elements used are those observed on the best maps available. However, stream network depiction is highly dependent on map scale and

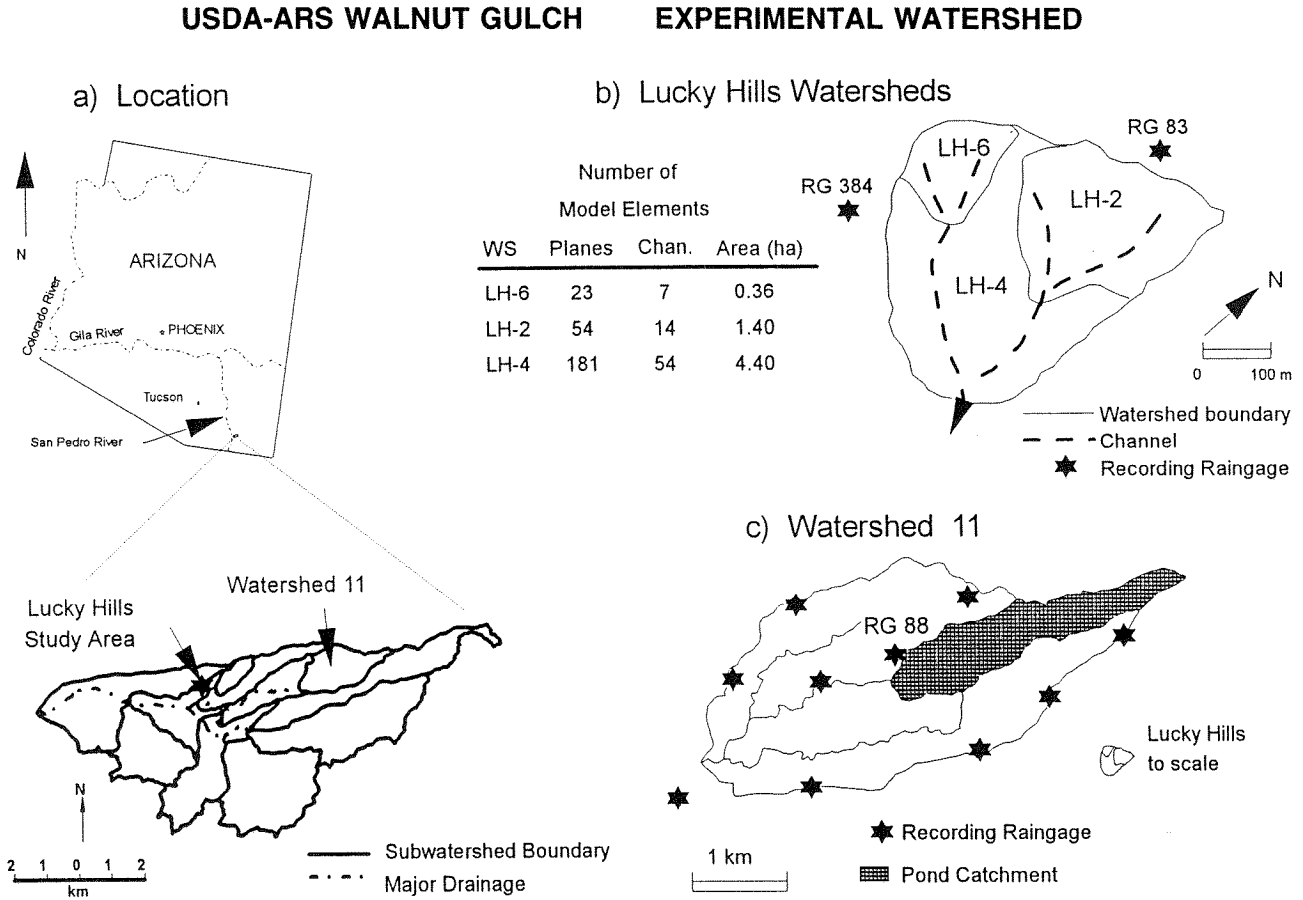

Fig. 20.6. a) Study area location map; b) Lucky Hills Watersheds; and c) Watershed 11.

cartographic judgement. This problem was addressed in Goodrich et al. (1988) and Goodrich (1991). It was concluded that an average channel support area of 15% (the average area upstream of channel initiation) was adequate to preserve model simulation of surface runoff for watersheds from 1.4 to 631 ha. Along with this it should be emphasized that high levels of discretization are not justified without having spatially distributed rainfall data of a commensurate detail.

Infiltration parameters (K_s) were estimated from soil texture analysis of 17 soil samples. Manning's roughness values (n) were estimated from the KINEROS User's Manual table 5 (Woolhiser et al., 1990a). Input rainfall data were obtained from raingage 83 for both LH-6 and LH-2 for the pretreatment split sample test. Pre-storm initial soil moisture conditions were calculated with the daily water balance component of the chemical transport model CREAMS (USDA, 1980).

For each of the watersheds, 10 pretreatment events were selected covering a large range of event sizes, initial conditions, and complexity of rainfall patterns. To decrease the optimization parameter space, it was assumed that the relative local values of K_s and n estimated from field measurements were fixed, and parameter multipliers were optimized. The Nash-Sutcliffe coefficient of efficiency (E), discussed above was used as an objective function for event runoff volume and peak runoff rate. When final multipliers were applied to initial field estimated parameters, the resulting values were checked to insure that they were physically realistic and were not acting as mere fitting parameters. These calibrated parameter sets were then used to model runoff response for an independent verification event set of 30 pretreatment events. Note that by using nested watersheds LH-6 and LH-2 within watershed LH-4, internal model verification was possible and some degree of interior, or distributed, model confidence could be established.

Using the optimum parameters, the KINEROS model performed very well as judged by the efficiency statistic (E) for both calibration and verification event sets on LH-6 and LH-2 (see columns labelled 1 in Table 20.1). Extrapolation capability is demonstrated by the simulation of runoff from events outside the calibration range of observed runoff volumes (0.8 to 14.5 mm) to a verification range of 0.3 to 47.5 mm. Typical scatter plots for calibration and verification events sets of simulated runoff volumes versus observed data are illustrated in Fig. 20.7 for pretreatment LH-6 events.

The favorable pretreatment modeling results encouraged use of the model for possible detection of hydrologic changes due to post-treatment vegetation changes. The ensuing analysis, described in more detail by Woolhiser et al. (1990b) demonstrated that due to model bias, predicting a

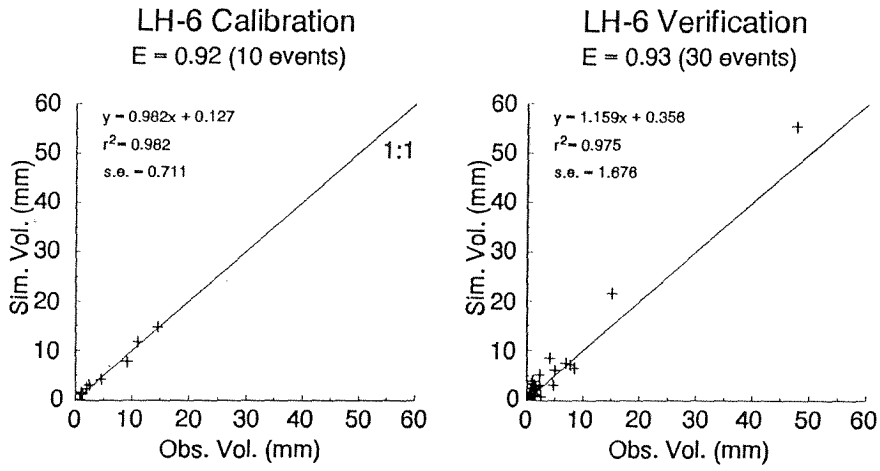

Fig. 20.7. Scatter plots for KINEROS calibration and verification for runoff volume on LH-6 for pretreatment conditions (1973-1980).

TABLE 20.1.

KINEROS calibration and verification coefficient of efficiency (E) for runoff volume (mm) and peak discharge (mm/hr) using optimum multipliers for the pretreatment period (1973-1980).

Basin		Calibration Efficiency				Verification Efficiency			
	Area	Volume		Peak		Volume		Peak	
	ha	1	2	1	2	1	2	1	2
LH-6	0.36	.92	.98	.93	.95	.93	.98	.77	.79
LH-2	1.40	.92	.97	.95	.97	.84	.93	.79	.93
LH-4	4.40	–	.96	–	.88	–	.99	--	.96

1 - one raingage. no heterogeneity

2 - two raingages, rainfall interpolation, small scale K_S heterogeneity

change in hydrologic regime can be misleading if model parameters were estimated from a small subset of pretreatment runoff data, and if the changes in runoff volumes are small. When the model bias for the treated watershed was accounted for by comparing results to the adjacent untreated LH-2 watershed, an apparent, but small, decease in runoff volumes was indicated due to enhanced infiltration on the treated and seeded LH-6 watershed.

However, this bias could not have been detected without the availability of paired watershed data. This analysis supports the results of Langford and McGuinness (1976) who found that the standard error of estimate for a model applied to a single watershed is greater than for comparison of paired watersheds.

Additional split sample testing, described in Goodrich (1991), was conducted on all three Lucky Hills watersheds (LH-2, LH-4, and LH-6) with a modified version of the model that incorporated several new features, some of which will be incorporated in the next release version (see section 4). These special features included representation of small scale variability of saturated hydraulic conductivity within a model element [(see Woolhiser and Goodrich (1988); Goodrich (1991); and Smith et al., 1990 for more detail)], and the space-time rainfall interpolation method to utilize multiple raingage information (described in section 20.4, below). As in the analysis above the calibration event set was selected to cover a range of runoff volume and intitial mositure conditions. The verification set contained events outside the calibration range to test model authenticity. For the Lucky Hills examples, rainfall data were obtained from raingage 83 and 384 which are separated by roughly 300m. An additional parameter, the coefficient of variation of saturated hydraulic conductivity, $C_v(K_s)$, was used during this optimization.

The results are summarized in the column labelled "2" in Table 20.1. Observed best and worst calibration simulation hydrographs for LH-4 are illustrated in Fig. 20.8. Timing errors of approximately eight to ten minutes or less are irrelevant in the Lucky Hills data, owing to normal clock errors. The better simulations occur for the largest events, and the worst occur for the smallest events for all watersheds. For the very small events, uncertainty of measurement error can become a large percentage of the observed runoff. The nonlinearities in the infiltration process will aslo tend to dominate the rainfall-runoff transformation. In all cases, the rainfall interpolation and K_s variability algorithms improved model results. Further analysis demonstrated that the majority of the improvement as measured by E came from using the additional raingage. Sensitivity to changes in C_v were particularly acute for small to medium events where the rainfall rates interact with spatially variable infiltration capacities. However, these events do not influence the E statistic to a large extent. For large events the variation in K_s (and therefore infiltration capacities) is largely overwhelmed by high rainfall intensities. Internal model consistency was demonstrated by successful application of the parameters from LH-4 to watersheds LH-2 and LH6, with E values from 0.86 to 0.97.

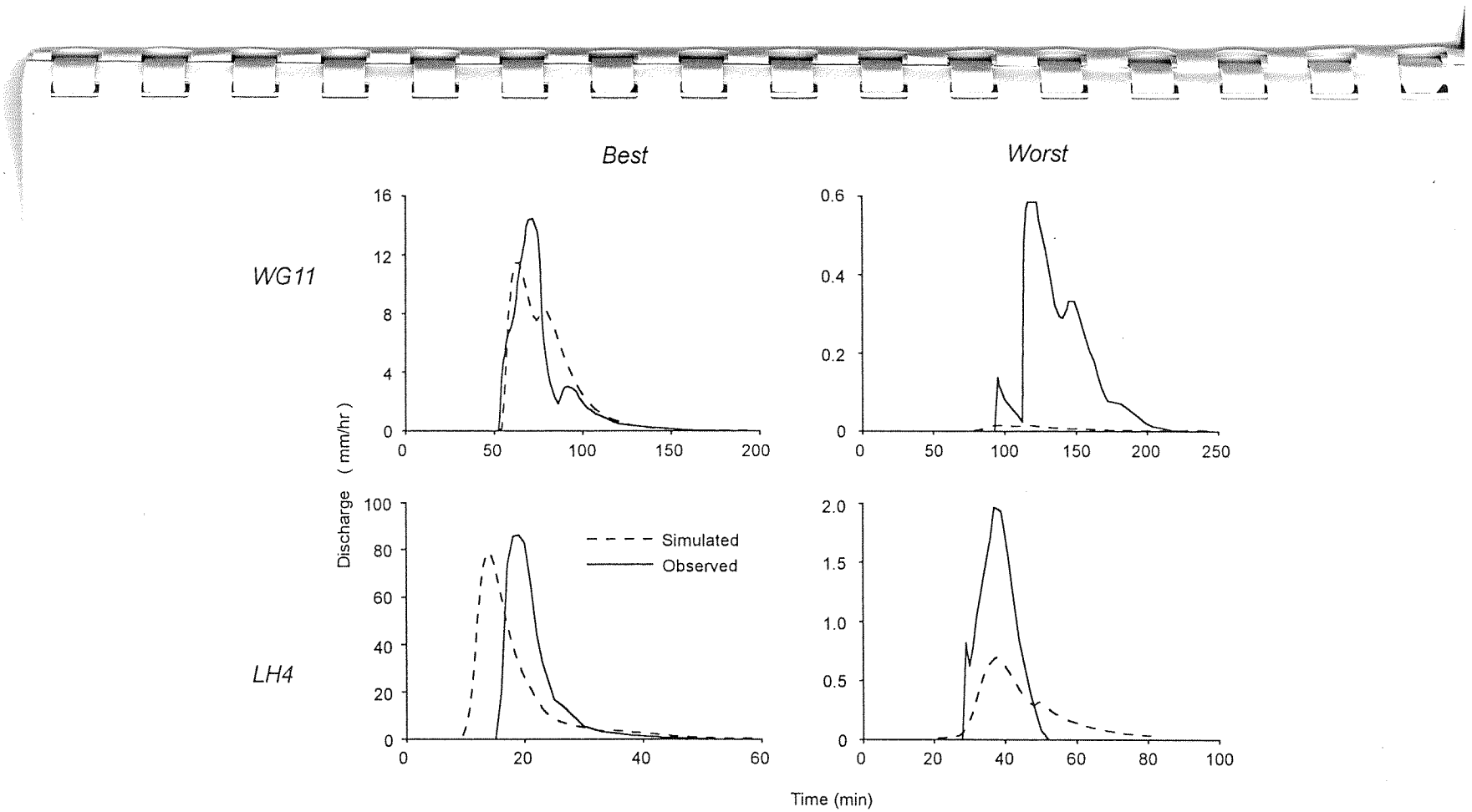

Fig. 20.8. Best and Worst sample hydrographs from calibration of the LH4 and WG11 watershed simulations.

20.3.3. Application to Large Semiarid Watersheds

Application of KINEROS to a larger subwatershed within Walnut Gulch (Watershed 11) and the entire basin has also been undertaken. Goodrich (1991) extended the analysis from the Lucky Hills watersheds discussed in the previous section to Watershed 11 (WG11 is 630 ha without the pond subcatchment, see Fig. 20.6). As in the Lucky Hills watersheds, parallel split sample testing with verification events outside the calibration range was conducted on WG11. Rainfall resolution requirements were also investigated. WG11 is characterized by mixed grasses, low shrub cover, and ephemeral stream channels with coarse sand beds that typically abstract a significant amount of runoff. The primary soils have a sandy loam texture and high surface rock content. Final infiltration rates range from 10 to 13 mm/hr and channel bed abstraction rates are as high as 225 mm/hr (Renard, 1970). Rainfall input is obtained via a space-time rainfall interpolation scheme (discussed below) from ten raingages located in and around the subwatershed.

As in the Lucky Hills application, ten calibration events with a range of rainfall amounts and antecedent soil moisture conditions were used to adjust the same basin-wide parameter multipliers. The optimum parameter set modeled the calibration event set with a coefficient of efficiency (E) for runoff volume of E = 0.86. For 20 independent verification events the efficiency dropped to E = 0.49. Scatter plots of the observed versus simulated runoff volumes for the calibration event set using 10 raingages are presented in Fig. 20.9.

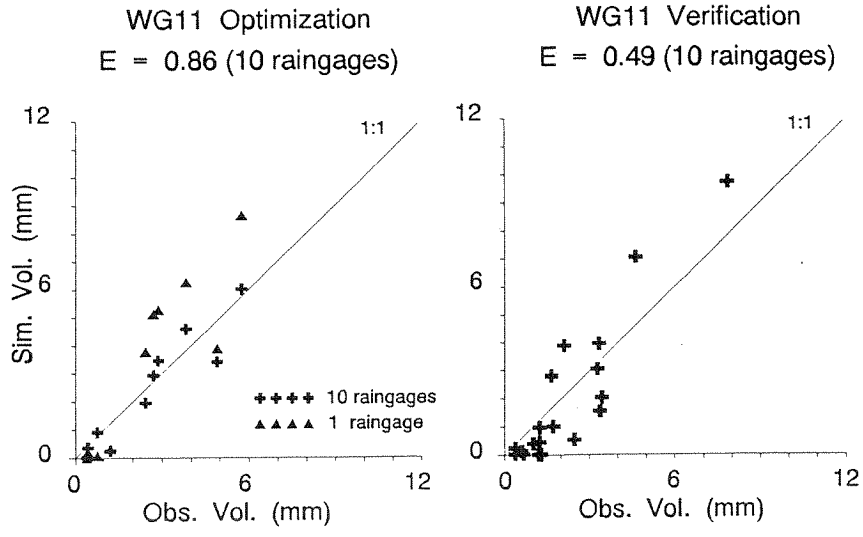

Fig. 20.9. Walnut Gulch Watershed 11 calibration and verification for runoff volume (10 raingages) and calibration set with 1 raingage.

Observed and best and worst simulation hydrographs (based on runoff volume) for the calibration event set are illustrated in Fig. 20.8. As in Lucky Hills the worst simulations occur for the smallest events.

Possible explanations for the model's poorer performance with the verification set include differing channel losses and antecedent soil conditions, and large random rainfall variability that may not have been captured in the small subset of ten calibration events in contrast to Lucky Hills examples. In addition, the same degree of field sampling to estimate initial parameters was not possible in the much larger WG11 watershed. However, the results cannot be dismissed outright as being unacceptable and are good when compared to other modeling efforts with Walnut Gulch data (Hughes and Beater, 1989).

To assess the impacts of spatial rainfall representation, the same events were simulated using data from a single raingage (RG 88) located near the center of WG11 (see Fig. 20.6). Use of a single raingage implies a spatially uniform rainfall representation. In Fig. 20.9, the modeled runoff volumes for the single raingage are also plotted. The figure illustrates that for 6 of 10 of the calibration events, and for all of the medium to large events, the uniform representation overestimated runoff volume (from 14 to 93%). In addition, the coefficient of efficiency for runoff volume dropped to 0.07. Because peak runoff rate is highly correlated with runoff volume in the semi-arid environment of Walnut Gulch (Goodrich, 1991), similar impacts on peak runoff rate occurred when the single raingage was used instead of the ten-gage network. This suggests that at the scale of WG11, the uniform rainfall representation results in poor estimations. Based on records from the dense raingage network on Walnut Gulch, runoff producing rainfall usually is restricted to only portions of the subwatersheds, and is not evenly distributed. This justifies the need for distributed rainfall representation within the model.

Michaud and Sorooshian (1992) applied KINEROS to the entire 15,000 ha Walnut Gulch Watershed. The primary objective of their study was to evaluate the accuracy of KINEROS simulations from a flash flood forecasting perspective under data constraints that are typical of watersheds with "ALERT" (Automated Local Evaluation in Real Time) flood warning systems. This limits the rain data to 1 gage per 2000 ha. KINEROS simulations were also compared to two SCS curve number models, lumped and distributed (McCuen, 1982), for "ungaged" and calibrated cases.

To match typical ALERT raingage density, only 8 recording raingages were used. Six calibration and 24 verification events were selected from the largest storms on record. However, 8 of the 24 verification events were from conventional streamflow measurements before a special supercritical flume was installed and the data from these events are of questionable quality. Instead of the rainfall interpolation scheme described below, they used kriging methods for interpolation. Small scale variability of saturated hydraulic conductivity (K_s) within model elements was also employed.

In general, they found that KINEROS was "reasonably accurate in simulating time to peak, but provides poor simulations of peak flow and runoff volume." This conclusion was supported by the E statistics for 24 verification events presented in Table 20.2 (from table 4-3 of Michaud and Sorooshian, 1992). The spatially-lumped SCS model could not accurately simulate flood peak and time to peak. For the calibration case, the distributed SCS model with channel losses was approximately as accurate as KINEROS. For the ungaged, or uncalibrated case, KINEROS was more accurate than the distributed SCS model. The major reasons cited for poor KINEROS runoff simulations were poor estimation of rainfall and prediction of infiltration. Roughly 50% of the simulation error was attributed to the coarse rainfall sampling.

TABLE 20.2.

KINEROS Nash-Sutcliffe efficiency for 24 verification events for the entire Walnut Gulch Watershed (from table 4-3 of Michaud and Sorooshian, 1992).

Case	Peak Rate	Runoff Volume	Time to Peak
Ungaged	-0.15	-0.52	0.91
Calibrated	-0.68	-0.39	0.78

20.3.4. Discussion of Applications

For the applications examined, KINEROS does a relatively good job simulating runoff and sediment yield at watershed scales of up to approximately 1000 ha (Zevenbergen and Peterson, 1988; Woolhiser et al., 1990b; and Goodrich, 1991). Distributed (interior) model accuracy was demonstrated within small (5 ha, 0.05 km^2) nested subwatersheds. Confidence in model accuracy at this scale highlighted an additional beneficial model use as a tool for data checking. Extremely poor simulation results prompted closer examination of the original rainfall and runoff gage charts. In numerous cases, errors in gage instrumentation or errors in data processing, such as improper time corrections were detected. For watersheds larger then 1000 ha, application of a detailed, process based model, such as KINEROS, may be difficult to justify in the absence of distributed rainfall data, given comparable results from a simpler model which does not entail the costs associated with detailed basin characterization required for KINEROS model inputs (Michaud and Sorooshian, 1992). But this assessment implies the existence of good data for proper calibration, and comparison of calibrated models.

20.4. IMPROVEMENTS UNDERWAY

A comprehensive revision of the FORTRAN program has recently been completed in anticipation of a second release (tentatively called KINEROS2) in 1994. The new code has a more consolidated, modular structure and includes the following additional capabilities:

(1) A composite "urban" element has been developed to mitigate the complexity of modeling an urban environment;

(2) The open channel algorithm has been extended to allow a compound cross section with an overbank section where hydraulic and infiltration parameters can differ from those in the main section;

(3) The new reservoir routing routine accounts for seepage through the wetted area, rainfall on the reservoir itself, and initial storage;

(4) The program will now synthesize rainfall input for individual elements using data from a network of raingages;

(5) The new infiltration model uses a new soil-physics based method for treating redistribution of water during any interruption in the storm, and will treat a soil profile comprised of two soil layers;

(6) A base flow can be specified for each open channel element;

(7) Time varying inflow from sources outside the model, such as measured flows or output from other models, can be injected into the modeled system at any point;

(8) Optional graphical output at the end of simulation showing the rainfall pattern and hydrograph simulated on any element;

(9) Soil and sediment are characterized by a distribution of up to 5 particle size classes rather than a single median particle size.

The composite urban element consists of four components: an open curbside gutter, an impervious area connected directly to the gutter, an impervious area contributing to a pervious area, and the pervious area which empties into the gutter. An interpretation of the element components as they might relate to a residential lot is shown in Fig. 20.10. The fraction of total area assigned to each component defines the element along with the hydraulic and infiltration parameters.

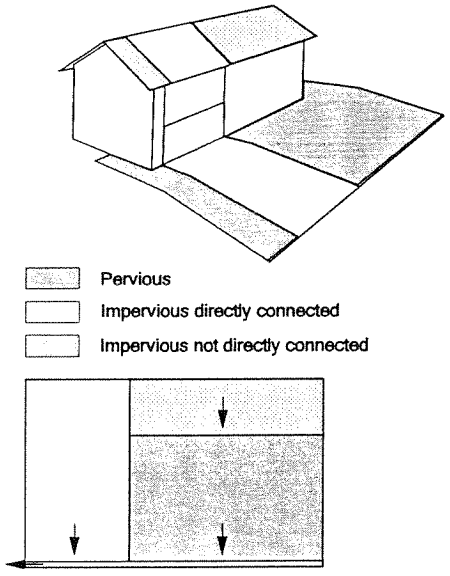

Fig. 20.10. Interpretation of an urban element in the new KINEROS2 model.

The compound channel algorithm is based on two independent kinematic equations - one for the main channel and one for the overbank section - that are written in terms of the same datum for flow depth. In writing the separate equations, it is explicitly assumed that no energy transfer occurs between the two sections, and upon adding the two equations the common datum implicitly requires the water surface elevation to be equal in both sections (Fig. 20.11). Each section has its own set of parameters describing

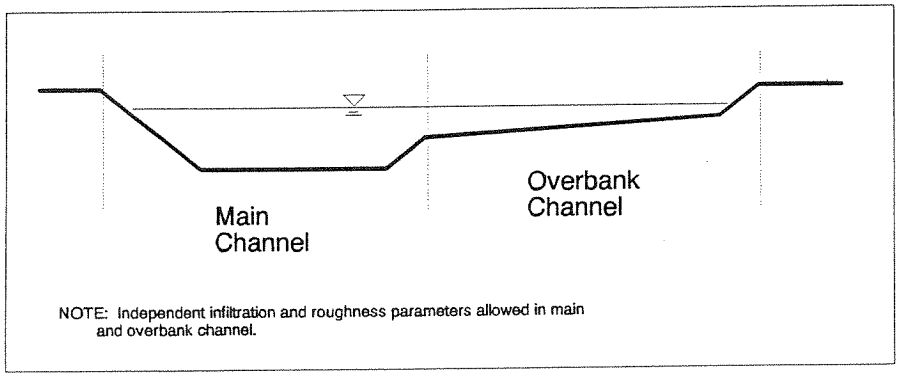

Fig. 20.11. Compound channel cross-section diagram in KINEROS2.

the hydraulic roughness, bed slope, and infiltration characteristics. A compound channel element can be linked with other compound channels or with simple trapezoidal channel elements.

Spatial relationships between raingages and model elements are expressed by rules based on proximity. The position of an element relative to the raingage network is described by a representative point such as the centroid of its area. If this point lies within the triangle formed by the three nearest raingages (in the xy plane), it is projected up to the plane passing through the intensity (z) at each raingage to obtain an interpolated intensity (Fig. 20.12a). If the representative point is not within this triangular region but lies within an area bounded by two parallel lines which pass through the

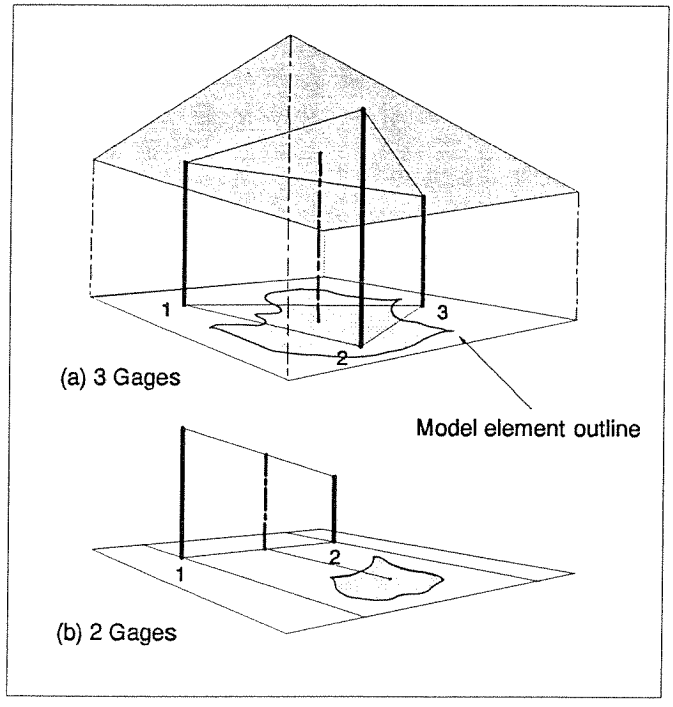

Fig. 20.12. Interpolation of rainfall intensity to element centroid.

two nearest raingages and are perpendicular to a line segment connecting the two raingages, the point is projected to the line segment and the intensity is linearly interpolated according to the relative position of the projected point on the line (Fig. 20.12b). If neither of these two conditions are met breakpoint data from the nearest raingage are used exclusively.

The breakpoint times from the two or three contributing raingage data sets are combined to define the time sequence for computing these intensities. The piece-wise planar (3 gages) or linear (2 gages) approximation of the rainfall intensity field is recomputed each time any

raingage intensity changes. The intensity interpolated at the runoff model element centroid is applied uniformly over the entire element. Therefore, the efficacy of the scheme becomes questionable if the model elements are large enough to encompass more than three raingages, because the resulting rainfall input will reflect data from at most three raingages and will neglect rainfall input from the other gages.

The new soil water profile simulation method allows input of a complex pattern of intensity, with multiple storms or significant rainfall hiatus. This method was developed by extending the infiltration model to include very high initial water contents, tracking secondary wetting fronts, and formulating an approximate simulation of redistribution based on soil hydraulic characteristics (Smith, et al, 1993). The two-layer soil model allows study of such natural phenomena as porous channel alluvium overlying a subsoil, and surface layers or crusted soils. Treatment of several sediment size classes allows realistic simulation of a watershed composed of eroding surface soils feeding alluvial channels comprised of different particle sizes, and allows a comparison of particle size distributions at the source and at the watershed outlet.

REFERENCES

Barnes, H.H., Jr. 1967. Roughness characteristics of natural channels. U.S. Geological Survey Water Supply Paper 1849, 213 pp.

Bennett, J.P. 1974. Concepts of mathematical modeling of sediment yield. *Water Resources Research* **10**(3):485-492.

Chow, V.T. 1959. *Open Channel Hydraulics*. 680 pp. McGraw-Hill, New York.

Dickinson, W.T., M.E. Holland, and G.L. Smith. 1967. An Experimental Rainfall-Runoff Facility. Hydrology Paper No. 25, Colorado State University, Fort Collins, CO, 81 pp.

Fair, G.M., and J.C. Geyer. 1954. *Water Supply and Wastewater Disposal.* 973 pp. John Wiley and Sons, New York.

Glass, L.J., and E.T. Smerdon. 1967. Effect of rainfall on the velocity profile in shallow-channel flow. *Transactions of the American Society of Agricultural Engineers* **10**(3):330-332, 336.

Goodrich, D. C., 1991. Basin scale and runoff model complexity. Univ. of Arizona, Dept. of Hydrology and Water Resources Tech. Rep. No. HWR 91-010, 361 p.

Goodrich, D.C., D.A. Woolhiser, and S. Soorooshian. 1988. Model complexity required to maintain hydrologic response. Proceedings, 1988 National Conf. of the Hydraulics Division, American Society of Civil Engineers, Colorado Springs, CO, Aug 8-12, pp.431-436.

Hughes, D. A., and Beater, A. B. (1989). The applicability of two single event models to catchments with different physical characteristics. *Hydrologic Sciences Journal*, **34**(1/2):63-78.

Julien, P.Y., and D.B. Simons. 1985. Sediment transport capacity of overland flow. *Transactions of the American Society of Agricultural Engineers* **28**(3):755-761.

Kibler, D.F., and D.A. Woolhiser, 1970. The kinematic cascade as a hydrologic model. Hydrology Paper No. 39. Colorado State University, Fort Collins, CO. 27 pp.

Lane, L.J., D.A. Woolhiser, and V. Yevjevich. 1975. Influence of simplifications in watershed geometry in simulation of surface runoff. Hydrology paper No. 81, Colorado State University, Fort Collins, CO. 50 pp.

Langford, K. J., and J. L. McGuinness, 1976. A comparison of modeling and statistical evaluation of hydrologic change. *Water Resources Research*, **12**(6):1322-1323.

Li, Ruh-Ming. 1972. Sheet flow under simulated rainfall. M.S. thesis, 111 pp., Colorado State University, Fort Collins.

McCuen, R. H., 1982. A Guide to Hydrologic Methods Using SCS Methods, Prentice Hall, Englewood Cliffs, N.J., 145 p.

Meyer, L.D., and W.H. Wischmeier. 1969. Mathematical simulation of the process of soil erosion by water. *Transactions of the American Society of Agricultural Engineers* **12**(6):754762.

Michaud, J.D. 1992. Distributed rainfall-runoff modeling of thunderstorm generated floods: A case study in a mid-sized semiarid watershed in Arizona. PhD. Dissertation, Univ. of Arizona, Tucson.

Michaud, J. D., and S. Sorooshian, 1992. Rainfall-runoff modeling of flash floods in semi-arid watersheds. Univ. of Arizona, Dept. of Hydrology and Water Resources Tech. Rep. No. HWR 92-030, 319 p.

Morgali, J.R. 1970. Laminar and turbulent overland flow hydrographs. *Journal of the Hydraulics Division*, American Society of Civil Engineers **91**(HY2):441-460.

Morris, E.M., and D.A. Woolhiser. 1980. Unsteady one-dimensional flow over a plane: Partial equilibrium and recession hydrographs. *Water Resources Research* **16**(2):355-360.

Nash, J. E. and J. V. Sutcliffe, 1970. River flow forecasting through conceptual models, I. A discussion of principles. *Journal of Hydrology*. **10**:282-290.

Rawls, W.J., D.L. Brakensiek, and K.E. Saxton. 1982. Estimation of soil water properties. *Transactions of the American Society of Agricultural Engineers* **25**(5):1316-1320, 1328.

Renard, K. G. 1970. The hydrology of semiarid rangeland watersheds. USDA-ARS pub. 41162.

Rovey, E.W. 1974. A kinematic model of upland watersheds. M.S. Thesis, Colorado State University, Fort Collins, 119 pp.

Rovey, E.W., D.A. Woolhiser, and R.E. Smith. 1977. A distributed kinematic model of upland watersheds. Hydrology Paper No. 93, Colorado State University, 52 pp.

Singh, V.P. 1974. A nonlinear kinematic wave model of surface runoff. PhD. Dissertation, Colorado State University, Fort Collins, CO. 282 pp.

Smith, R.E. 1982. Rational models of infiltration hydrodynamics. *In Modeling Components of Hydrologic Cycle,* Water Resources Publications, Littleton, CO, pp. 107-126.

Smith, R.E. 1983. Flux infiltration theory for use in watershed hydrology. *In Proceedings of the National Conference on Advances in Infiltration*, pp. 313-323, American Society of Agricultural Engineers, St. Joseph MI.

Smith, R.E., C. Corradini, and F. Melone. 1993. Modeling infiltration for multistorm runoff events. *Water Resources Research* **29**(1):133-144.

Smith, R.E., and J.-Y. Parlange. 1978. A parameter-efficient hydrologic infiltration model. *Water Resources Research* **14**(3):533-538.

Smith, R. E., D. C. Goodrich, and D. A. Woolhiser, 1990. Areal effective infiltration dynamics for runoff on small catchments. Trans. 14th Inter. Congress of Soil Sci., Volume I: Commission I, p. 22-27, August, Kyoto, Japan.

Unkrich, C.L., and H.B. Osborn. 1987. Apparent abstraction rates in ephemeral stream channels. *Hydrology and Water Resources in Arizona and the Southwest*, Offices of Arid Land Studies, University of Arizona, Tucson, **17**:34-41.

USDA. 1980. CREAMS: A Field-scale model for chemicals, runoff, and erosion from agricultural management systems. Knise, W.G., ed. U.S. Department of Agriculture Conservation Research Report No. 26, 640 pp.

Woolhiser, D. A. and D. C. Goodrich. 1988. Effect of storm rainfall intensity patterns on surface runoff. *Journal of Hydrology*, (102):335-354.

Woolhiser, D.A., C.L. Hanson, and A.R. Kuhlman. 1970. Overland flow on rangeland watersheds. *Journal of Hydrology (New Zealand)* **9**(2):336-356.

Woolhiser, D.A., M.E. Holland, G.L. Smith, and R.E. Smith. 1971. Experimental investigation of converging overland flow. *Trans. ASAE* **14**(4):684-687.

Woolhiser, D.A., R.E. Smith, and D.C. Goodrich. 1990a. KINEROS, A Kinematic Runoff and Erosion Model: Documentation and User Manual. U.S. Dept. of Agriculture, Agricultural Research Service, ARS-77, 130 pp.

Woolhiser, D. A., D. C. Goodrich, W. E. Emmerich, and T. O. Keefer, 1990b. Hydrologic effects of brush to grass conversion. Proc. ASCE Nat. Conf. on Irrig. and Drain., Durango, CO, p. 293-302, July 11-15.

Woolhiser, D.A., and J.A. Liggett. 1967. Unsteady, one-dimensional flow over a plane-the rising hydrograph. *Water Resources Research* **3**(3):753-771.

Wu, Y-H, V. Yevjevich, and D.A. Woolhiser. 1978. Effects of surface roughness and its spatial distribution on runoff hydrographs. Hydrology Paper No. 96, Colorado State University, Fort Collins, CO. 47 pp.

Yu, Y.S., and J.S. McNown. 1964. Runoff from impervious surfaces. *Journal of Hydraulic Research* **2**(1):3-24.

Zevenbergen, L. W., and M. R. Peterson, 1988. Evaluation and testing of storm-event hydrologic models. Proc. ASCE Nat. Conf. on Hydraulic Engr., Colo. Springs, CO, Aug. 6-12., p. 467472.